THE JOURNAL OF PHYSICAL CHEMISTRY A

Article

pubs.acs.org/JPCA

Evolution of Electric Dipole (Hyper)polarizabilities of β-Strand Polyglycine Single Chains: An ab Initio and DFT Theoretical Study

Andrea Alparone*

Department of Chemistry, University of Catania, viale A. Doria 6, Catania -95125, Italy

ABSTRACT: Ab initio and density functional theory calculations have been carried out on dipole moments (μ), polarizabilities (α), and second-order hyperpolarizabilities (γ) of single chain β-strand oligoglycines in the gas phase. Basis set and electron correlation effects have been investigated. The long-range corrected CAM-B3LYP and ωB97X-D functionals furnish satisfactory results in agreement with correlated ab initio computations. The dependence of μ, α, and γ values per unit cell on chain length has been explored, extrapolating the properties in the limit of the polymer. The increase of the response electronic properties with the number of glycine units has been rationalized through the two-state model involving the typical $\pi-\pi^*$ NV_1 electronic transition of peptides. The effect of the secondary structure on the electric properties has been discussed. At variance from the dipole moments, the γ values increase on going from the α-helices to the β-strands, whereas the α values are little influenced by the conformation of the oligoglycines.

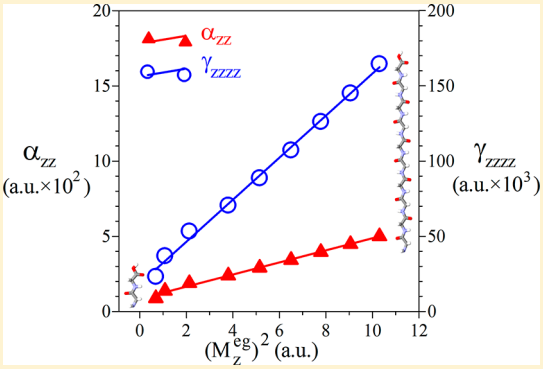

1. INTRODUCTION

Organic nonlinear optical (NLO) compounds have drawn great attention in the past decades toward design and application of photonic and electro-optical materials.[1,2] Polymers based on delocalized π-electron systems exhibit large NLO responses, being promising candidates for the fabrication of efficient optoelectronic devices.[2−4] In recent years, the center of attention for novel conductive and NLO materials has been directed toward biomolecules, which are easily accessible in nature. Structures based on peptide fragments are currently employed for the development of NLO devices.[5] Theoretical investigations on oligoglycines attached to gold nanoelectrodes have evidenced that these systems show diode properties, being potentially suitable for constructing electric conductors.[6,7] Owing to the presence of strong polar groups, polypeptides are often highly polar systems,[8−12] an advantageous characteristic for fabrication of NLO poled-polymers.[3] Another interesting property of polypeptide chains is that they absorb rather far from the visible region (~6.5 eV),[13] which is of crucial importance to optimize transparency-optical nonlinearity trade-off.[14,15]

NLO response properties may be strongly affected by structural features and are of potential utility to identify molecular conformations.[16,17] Second harmonic generation and sum frequency generation phenomena are currently used to characterize structures of biomolecules such as peptides and proteins.[18−23] Electric susceptibility of glycine-based peptides were employed to describe conformational, folding, and zwitterionic states.[24,25] First-order hyperpolarizabilities of the naturally occurring amino acids phenylalanine, tryptophan, tyrosine, and of the lysine−tryptophan−lysine tripeptide were measured through hyper-Rayleigh scattering NLO techniques.[26] On the theoretical side, NLO properties of small and large single- and multichain peptides, including polyglycines, were modeled by using additive schemes.[27−31]

Glycine oligomers are often employed in modeling physicochemical properties of more sizable oligopeptides. In the solid, polyglycines are prevalently present in two different conformations: polyglycine I with the typical Ramachandran dihedral angles $\varphi = -150°$ and $\psi = 147°$ and polyglycine II characterized by $\varphi = -77°$ and $\psi = 145°$.[32,33] However, in the gas phase, the lowest-energy single-chain oligoglycines are predicted to occur prevalently in α-helix or 3_{10}-helix secondary structural arrangements.[34−37] Wu and Zhao[37] computed the structures, energetics, and dipole moments of α-helices, 3_{10}-helices, 2_7-ribbons, and β-strand forms at the Hartree−Fock (HF) and density functional theory (DFT) using the B3LYP functional with the 6-31G* basis set. Geometries and stabilization energies of single-chain $H_2N-(CH_2-CO-NH)_n-CH_2COOH$ (n = 1−9) oligoglycines in the β-sheet conformation were previously obtained through B3LYP calculations.[38] Dipole moments, electronic polarizabilities, and Rayleigh depolarization ratios and activities of small sized oligoglycines were determined by Chaudhuri and Canuto using HF, B3LYP, and B3P86 methods.[39] Vertical ionization energies, electron affinities, and their differences for α-helix and β-strand oligoglycine conformations were calculated at DFT level using a ΔSCF procedure.[40] More recently, dipole moments and electronic (hyper)polarizabilities of single-chain α-helix oligo-

Received: March 30, 2013
Revised: May 28, 2013
Published: May 29, 2013

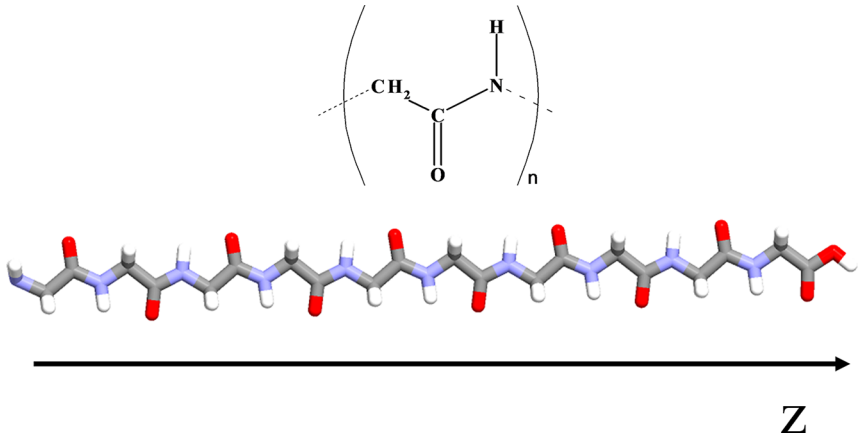

Figure 1. Structure of the $H_2N-(CH_2-CO-NH)_9-CH_2COOH$ β-strand conformation. Colors: gray (carbon), cyan (nitrogen), red (oxygen), and white (hydrogen).

glycines have been studied using the Coulomb-attenuating DFT method (CAM-B3LYP).[41]

The main goal in this work is to characterize the electric properties of single-chain oligoglycines $H_2N-(CH_2-CO-NH)_n-CH_2COOH$ (n = 1−9) in the β-strand form. Evolutions of the properties with the increase of the chain length have been explored, predicting the values in the limit of the polyglycine. The physicochemical properties of the β-strands have been compared to those of the corresponding α-helices recently obtained at the same level of calculation.[41] Dipole moments, static electronic polarizabilities, and second-order hyperpolarizabilities have been determined in the gas phase using ab initio HF, second-order Møller−Plesset perturbation theory (MP2), and DFT levels. As well-known in literature, the conventional DFT is inappropriate especially for (hyper)-polarizability computations of π-conjugated systems, often overestimating response electric properties obtained at correlated ab initio levels.[42] The inaccurate behavior is mainly caused from the so-called self-interaction error in the exchange part of the conventional functionals, failing to adequately predict response electric properties, which involve nonlocal phenomena. However, recent studies on small and large molecules have demonstrated that novel functionals based on long-range corrected potentials furnish good results in predicting electronic (hyper)polarizabilites, with improved performances over traditional functionals in reproducing high-level theoretical ab initio methods but with relatively less computational requirements.[41,43−58] The long-range corrected functionals incorporate certain contributions of exact HF exchange potential in the long-range interaction component, which are beneficial for the prediction of nonlocal effects.[43]

The present article is organized as follows. The computational methodologies are described in the next section. Then we discuss dipole moments, electronic polarizabilities, and second-order hyperpolarizabilities, comparing the properties of the β-strands with those of the corresponding α-helices. The conclusions are summarized in the last section.

2. COMPUTATIONAL DETAILS

All calculations were performed using Gaussian09[59] and GAMESS programs.[60] The geometries of the β-strand oligoglycines $H_2N-(CH_2-CO-NH)_n-CH_2COOH$ (n = 1−9) previously optimized at the B3LYP/6-311+G** level[38] were employed throughout this work. In order to reduce the computational demand, for each peptide, we imposed a planar C_s symmetry. The structures were oriented in the Cartesian frame with the z-axis directed along the principal axis of the chains (Figure 1).

Static electronic dipole polarizability (α_{ij}) and second-order hyperpolarizability (γ_{ijkl}) tensor components were calculated analytically at the HF level using the time-dependent HF procedure (TD-HF).[61,62] Electron correlation effects were introduced through the MP2 theory under the frozen-core approximation. As widely documented in literature, electronic (hyper)polarizabilities can be significantly influenced by introduction of electron correlation contributions.[63−69] The MP2 calculations were carried out numerically through a finite-field (FF) differentiation scheme using the Romberg procedure previously illustrated by Champagne and co-workers.[70,71] The FF computations were performed using field strength amplitudes ranging from 0.0008 to 0.0256 au. The accuracy of the numerical procedure was tested at the HF level, by comparing (hyper)polarizability data obtained by the FF-HF and TD-HF calculations. Additionally, for the smallest oligomer as a benchmark, we performed computations at higher electron correlation treatments, using the fourth-order Møller−Plesset perturbation theory with single, double, triple, and quadruple excitations (MP4-SDTQ), as well as the coupled cluster with single, double (CCSD), and triple excitations [CCSD(T)] methods. Besides the ab initio levels, we also explored the performances of the conventional B3LYP functional[72,73] and long-range corrected CAM-B3LYP[74] and ωB97X-D[75] DFT methods. The nature of the exchange-correlation DFT potential is crucial especially for hyperpolarizability calculations. Traditional gradient-corrected functionals such as the widely used B3LYP method, usually overestimate the electronic (hyper)polarizabilities obtained with correlated ab initio levels.[42] However, recent studies have demonstrated that the long-range corrected CAM-B3LYP and ωB97X-D methods give excellent performances for response electronic properties,[41,43−58] in particular reproducing adequately coupled-cluster (hyper)polarizability data of glycine conformations[56] and polyacetilene oligomers.[57]

Accurate predictions of electronic (hyper)polarizabilities need flexible basis sets containing diffuse and polarized functions.[76−79] There are many indications in literature showing that the 6-31+G* basis set, which includes polarized diffuse functions on the first-raw heavy atoms (carbon,

dx.doi.org/10.1021/jp403155q | J. Phys. Chem. A 2013, 117, 5184−5194

Table 1. Dipole Moments μ (D), Polarizabilities α (au), and Second-Order Hyperpolarizabilities γ (au) of β-Strand Oligoglycines $H_2N-(CH_2-CO-NH)_n-CH_2COOH$ (n = 1−9)

	μ_z	μ	α_{zz}	$\langle\alpha\rangle$	γ_{zzzz}	$\langle\gamma\rangle$	μ_z	μ	α_{zz}	$\langle\alpha\rangle$	γ_{zzzz}	$\langle\gamma\rangle$
	n = 1						n = 6					
HF/6-31G	2.717	2.985	66.19	54.84	7400	2332	12.800	12.803	258.72	187.53	49101	12422
HF/6-31+G*	2.645	2.872	77.47	64.62	12660	5907	12.903	12.913	293.54	216.96	60558	22408
HF/6-31++G**	2.600	2.827	78.66	65.54	12760	6488	12.814	12.826	298.18	219.81	63046	24720
HF/aug-cc-pVDZ	2.459		87.44		13555							
MP2/6-31+G*	2.953	3.146	88.85	71.39	23186	10318	14.689		343.37		107230	
MP4-SDTQ/6-31+G*	2.903	3.094	89.65	71.71	25413	11372						
CCSD/6-31+G*	2.839		86.55		22868							
CCSD(T)/6-31+G*	2.890		88.93		25949							
B3LYP/6-31+G*	2.886	3.065	93.03	73.19	39977	15793						
CAM-B3LYP/6-31+G*	2.889	3.077	89.43	71.46	26265	11408	14.487	14.490	343.85	241.85	122559	43410
ωB97X-D/6-31+G*	2.906	3.087	88.93	71.12	24857	11018	14.562		343.03		118155	
	n = 2						n = 7					
HF/6-31G	4.619	4.625	103.59	80.95	14150	4036	14.887	14.941	297.84	214.32	58498	14650
HF/6-31+G*	4.581	4.614	119.34	94.65	20603	8913	15.025	15.069	337.53	247.69	71240	25907
HF/6-31++G**	4.527	4.565	121.19	95.95	21104	9827	14.928	14.971	342.88	250.94	74327	28660
HF/aug-cc-pVDZ	4.376		134.80		21725							
MP2/6-31+G*	5.146		137.81		36922		17.130		395.44		126175	
CAM-B3LYP/6-31+G*	5.059	5.071	138.36	104.92	41409	17024	16.898	16.934	395.90	276.31	144678	50308
ωB97X-D/6-31+G*	5.086		137.80		40018		16.987		394.99		139636	
	n = 3						n = 8					
HF/6-31G	6.559	6.677	141.38	107.41	22152	5987	17.020	17.021	337.42	241.14	68001	16899
HF/6-31+G*	6.543	6.641	161.99	125.04	29975	12145	17.201	17.208	381.86	278.45	81924	29431
HF/6-31++G**	6.478	6.575	164.51	126.72	30953	13399	17.097	17.105	387.93	282.09	85692	32665
HF/aug-cc-pVDZ	6.322		183.30		31687							
MP2/6-31+G*	7.416		188.51		53320		19.615		447.87		145142	
CAM-B3LYP/6-31+G*	7.293	7.373	188.61	138.89	60043	23215	19.358	19.360	448.30	310.81	166832	57251
ωB97X-D/6-31+G*	7.333		187.97		58063		19.459		447.35		160672	
	n = 4						n = 9					
HF/6-31G	8.633	8.636	180.44	134.03	30795	8064	19.131	19.174	376.57	267.76	77501	19140
HF/6-31+G*	8.660	8.676	205.69	155.59	39782	15504	19.349	19.384	425.87	309.01	92735	32943
HF/6-31++G**	8.588	8.606	208.91	157.66	41226	17109	19.237	19.272	432.65	313.05	96872	36284
HF/aug-cc-pVDZ	8.436		232.89		41372							
MP2/6-31+G*	9.825		239.54		70572		22.083		499.98		164582	
CAM-B3LYP/6-31+G*	9.679	9.684	240.06	173.09	79909	29793	21.797	21.825	500.40	345.11	189335	64336
ωB97X-D/6-31+G*	9.730		239.37		77355		21.910		499.34		182735	
	n = 5											
HF/6-31G	10.688	10.762	219.27	160.69	39818	10214						
HF/6-31+G*	10.747	10.809	249.37	186.18	50122	18926						
HF/6-31++G**	10.666	10.727	253.29	188.64	52057	20878						
MP2/6-31+G*	12.229		291.16		88715							
CAM-B3LYP/6-31+G*	12.051	12.101	291.67	207.35	101050	36432						
ωB97X-D/6-31+G*	12.115		290.90		97681							

nitrogen, and oxygen), is a suitable choice for (hyper)-polarizability computations of relatively large molecules, producing values close to those obtained with much more extended basis sets,[41,57,80−82] but with minor computational resources. However, we explored the basis set effects on the electric properties at the HF level using a hierarchy of basis sets such as 6-31G, 6-31+G*, 6-31++G**, and aug-cc-pVDZ.

In the present study, besides the longitudinal components along the z-axis direction, we also report the dipole moment (μ), average polarizability ($\langle\alpha\rangle$), and average second-order ($\langle\gamma\rangle$) hyperpolarizability invariants, which are defined as

$$\mu = \sqrt{\mu_x^2 + \mu_y^2 + \mu_z^2} \tag{1}$$

$$\left\langle \alpha \right\rangle = \frac{1}{3}(\alpha_{xx} + \alpha_{yy} + \alpha_{zz}) \tag{2}$$

$$\left\langle \gamma \right\rangle = \frac{1}{5}[\gamma_{xxxx} + \gamma_{yyyy} + \gamma_{zzzz} + 2(\gamma_{xxyy} + \gamma_{xxzz} + \gamma_{yyzz})] \tag{3}$$

where i, j = x, y, z.

For the response electric properties, atomic units are used throughout the work. Conversion factor to the SI are 1 au of α ($e^2a_0^2E_h^{-1}$) = 1.648778×10^{-41} C^2 m^2 J^{-2}; 1 au of γ ($e^4a_0^4E_h^{-3}$) = 6.235377×10^{-65} C^4 m^4 J^{-3}.

3. RESULTS AND DISCUSSION

A. Dipole Moments. Table 1 lists the μ_z and μ values of the investigated oligoglycines as a function of the chain length n.

dx.doi.org/10.1021/jp403155q | J. Phys. Chem. A 2013, 117, 5184−5194

For all the peptides, μ_z is clearly the dominant component recovering ca. 94% and 99% of the total μ value for the oligomer with $n = 1$ and $n = 9$, respectively. The introduction of electron correlation at the CCSD(T) and MP2 levels increases the HF/6-31+G* μ_z datum of $H_2N-(CH_2-CO-NH)-CH_2COOH$ by 0.245 D (+9.3%) and 0.308 D (+11.6%), respectively. For the largest oligomers ($n = 2-9$), the effects of the electron correlation are also positive, the MP2/6-31+G* μ_z values being higher than the HF/6-31+G* data by 12−14%. All the DFT methods agree well with the MP2 μ_z data, with percentage deviations within 1−2%. The effects of the basis sets here evaluated at the HF level are somewhat modest (within ca. 4%).

Next, we focus our attention to the dependence of the dipole moments on the chain length. The β-strand polyglycines are very polar systems, the μ values rising steadily with the increase of the n value: at the CAM-B3LYP/6-31+G* level, the μ value for $H_2N-(CH_2-CO-NH)-CH_2COOH$ and $H_2N-(CH_2-CO-NH)_9-CH_2COOH$ is calculated to be 3.1 and 21.8 D, respectively. These values can be compared with the B3LYP/6-31G* data previously reported by Wu and Zhao[37] for $H_2N-(CO-CH_2-NH)_n-COCH_3$ peptides, which are 3.2 D ($n = 1$) and 20.4 D ($n = 9$). In addition, our CAM-B3LYP/6-31+G* μ data for $H_2N-(CH_2-CO-NH)_n-CH_2COOH$ with $n = 1$, 2, 3, and 4, which are computed to be 3.1, 5.1, 7.4, and 9.7 D, respectively, are in reasonable agreement with the B3LYP/6-31+G* values previously calculated by Chaudhuri and Canuto,[39] which are 3.2, 5.3, 7.7, and 9.0 D, respectively.

Figure 2 shows the evolution of the μ_z values per unit cell ($\Delta\mu_z$) as a function of the number of glycine units. Following

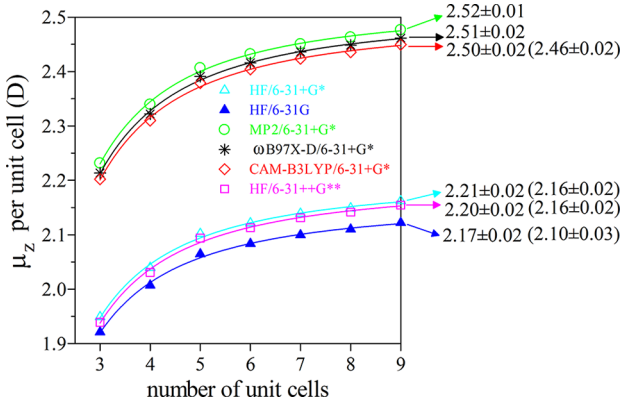

Figure 2. Calculated μ_z per unit cell $\{\Delta\mu_z = [\mu_z(n) - \mu_z(n-2)]/2\}$ of the $H_2N-(CH_2-CO-NH)_n-CH_2COOH$ ($n = 1-9$) oligomers as a function of the chain length. The reported data refer to the extrapolated properties in the limit of the polymer $\Delta\mu_z(n \rightarrow \infty)$. The value in parentheses refers to the $\Delta\mu(n \rightarrow \infty)$ datum.

previous studies on polymeric systems,[83,84] in order to minimize chain end effects, for $\Delta\mu_z$, we adopted the difference between the oligomers with n and $n-2$ units, $\Delta\mu_z = [\mu_z(n) - \mu_z(n-2)]/2$. Approximate estimates for $\Delta\mu_z$ in the limit of the polymer ($n \rightarrow \infty$) can be determined through the frequently used extrapolation fitting formula[85,86]

$$\Delta\mu_z = a + b/n + c/n^2 \quad (4)$$

where a, b, and c are least-squares fitting parameters. The extrapolated $\Delta\mu_z$ values in the limit of the polyglycine $[\Delta\mu_z(n \rightarrow \infty)]$, which are nearly provided by the a parameter, are given in Figure 2. The $\Delta\mu_z(n \rightarrow \infty)$ values confirm the excellent results for both the long-range corrected functionals, which reproduce the MP2 datum within 0.01−0.02 D (0.4−0.8%). In addition, by using the CAM-B3LYP/6-31+G* (HF/6-31+G*) μ values, the extrapolated $\Delta\mu(n \rightarrow \infty)$ datum is predicted to be 2.46 ± 0.02 D (2.16 ± 0.02 D), the $\Delta\mu_z(n \rightarrow \infty)/\Delta\mu(n \rightarrow \infty)$ ratio being close to unity.

B. Polarizabilities. The calculated polarizabilities for the $n = 1-9$ peptides are given in Table 1. Not surprisingly, α_{zz} is the dominant component for all the oligomers, amounting to ca. 50% of the total polarizability ($\alpha_{xx} + \alpha_{yy} + \alpha_{zz}$) for $H_2N-(CH_2-CO-NH)_9-CH_2COOH$. In agreement with common literature, introduction of electron correlation at the CCSD(T) and MP2 levels gives a positive contribution to polarizability, enhancing the HF/6-31+G* α_{zz} value of the oligomer with $n = 1$ by 11.46 au (+14.8%) and 11.38 au (+14.7%), respectively. This result demonstrates that, the MP2 level approximates reasonably well the CCSD(T) method, but with noticeably less computational costs. In consistency with recent studies,[41,43−58] the long-corrected functionals agree satisfactorily with the correlated ab initio methods: for the oligomer with $n = 1$, the CAM-B3LYP/6-31+G* α_{zz} value overestimates the corresponding CCSD(T)/6-31+G* datum by only 0.50 au (+0.6%), while the ωB97X-D/6-31+G* and CCSD(T)/6-31+G* α_{zz} values are identical. However, the conventional B3LYP functional overestimates the α_{zz} CCSD(T)/6-31+G* datum of $H_2N-(CH_2-CO-NH)-CH_2COOH$ by 4.10 au (+4.6%). Similar results are found on the larger peptides ($n \geq 2$), the CAM-B3LYP/6-31+G* (ωB97X-D/6-31+G*) reproducing the MP2/6-31+G* α_{zz} values within 0.1−0.7% (0.1%). Note that, for the largest oligomer, the introduction of the MP2 electron correlation effects increases the HF/6-31+G* α_{zz} value by ca. 17%. In addition, we explored the effects of the basis sets on the longitudinal and average polarizabilities obtained at the HF level. As can be appreciated from the data of Table 1, the introduction of polarized and diffuse functions on the heavy atoms (6-31G → 6-31+G*) increases the α_{zz} and $\langle\alpha\rangle$ values of $H_2N-(CH_2-CO-NH)-CH_2COOH$ by 11.28 au (+17.0%) and 9.78 au (+17.8%), respectively. Note that, for the oligoglycine with $n = 9$, the percentage deviations are smaller, being +13.1% and +15.4%, respectively. The further augmentation of the basis set (6-31+G* → 6-31++G**) produces a minor impact on the calculated polarizabilities, which increase within ca. 1%. For the smallest oligomers ($n = 1-4$), we compared the HF/6-31++G** and HF/aug-cc-pVDZ α_{zz} data. The results show that the basis set effects remain almost constant for all the peptides, the HF/aug-cc-pVDZ α_{zz} data being ca. 10% greater than the corresponding HF/6-31++G** values.

The present $\langle\alpha\rangle$ values can be compared with previous theoretical estimates available in the literature. Mochizuki et al.,[87] using the linear response method with the 6-31G** basis set, computed an $\langle\alpha\rangle$ value of 133.19 au for a helical-type conformation of $H_2N-(CH_2-CO-NH)_4-CH_2COOH$, which is close to our value obtained at the HF/6-31G level (134.03 au). In addition, the CAM-B3LYP/6-31+G* $\langle\alpha\rangle$ values for the oligomers with $n = 1$, 2, 3, and 4, which are calculated to be 71.46, 104.92, 138.89, and 173.09 au, respectively, agree well with those previously obtained by Chaudhuri and Canuto[39] at the B3P86/6-31+G* level (72.58, 106.80, 141.55, and 176.68 au, respectively).

As for the dipole moments, the α_{zz} value progressively increases with the increase of the chain length, the CAM-B3LYP/6-31+G* data ranging from 89.43 ($n = 1$) to 500.40 au

dx.doi.org/10.1021/jp403155q | J. Phys. Chem. A 2013, 117, 5184−5194

(n = 9). The corresponding $\langle\alpha\rangle$ values are calculated to be 71.46 and 345.11 au, respectively. Figure 3 illustrates the

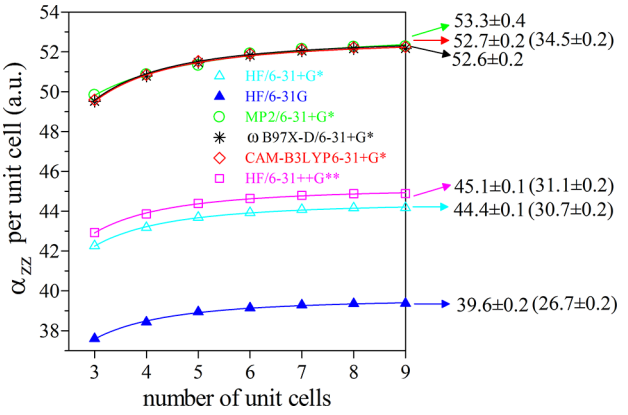

Figure 3. Calculated α_{zz} per unit cell $\{\Delta\alpha_{zz} = [\alpha_{zz}(n) - \alpha_{zz}(n-2)]/2\}$ of the $H_2N-(CH_2-CO-NH)_n-CH_2COOH$ (n = 1–9) oligomers as a function of the chain length. The reported data refer to the extrapolated properties in the limit of the polymer $\Delta\alpha_{zz}(n \rightarrow \infty)$. The value in parentheses refers to the $\Delta\langle\alpha\rangle(n \rightarrow \infty)$ datum.

evolution of the α_{zz} data per unit cell, $\Delta\alpha_{zz} = [\alpha_{zz}(n) - \alpha_{zz}(n-2)]/2$, as a function of n. By analogy to the calculated dipole moments, we determined the $\Delta\alpha_{zz}$ values for $n \rightarrow \infty$ [$\Delta\alpha_{zz}(n \rightarrow \infty)$], by adopting an extrapolation fitting formula similar to that of eq 4. The estimated $\Delta\alpha_{zz}(n \rightarrow \infty)$ values are inserted in Figure 3, confirming that both the long-range corrected functionals furnish good performances, with values close to the MP2 datum (up to 1.6–1.7 au, −3%). Additionally, when we use the CAM-B3LYP/6-31+G* (HF/6-31+G*) $\langle\alpha\rangle$ values listed in Table 1, the $\Delta\langle\alpha\rangle(n \rightarrow \infty)$ datum is estimated to be 34.5 ± 0.2 au (30.7 ± 0.2 au), whereas the $\Delta\alpha_{zz}(n \rightarrow \infty)/[3\Delta\langle\alpha\rangle(n \rightarrow \infty)]$ ratio is nearly independent of the basis set and level of calculation (0.49, 0.48, 0.48, and 0.51 for the HF/6-31G, HF/6-31+G*, HF/6-31++G**, and CAM-B3LYP/6-31+G*, respectively). It is worth noting that the $\Delta\alpha_{zz}$ and $\Delta\langle\alpha\rangle$ values for the largest oligomer converge toward the asymptotic values of the polyglycine (within 1–2%).

Molecular polarizabilities are frequently related to volumes through the well-known Clausius–Mosotti formulation [$\langle\alpha\rangle = 3(\varepsilon - 1)/4\pi(\varepsilon + 2)$ volume]. In the present study, we determined molar volumes (V) of the peptides at the HF/6-31+G* and CAM-B3LYP/6-31+G* levels through the Monte Carlo integration method implemented in the Gaussian09 package using 0.001 e/bohr^3 isodensity envelopes. Interestingly, the molar volumes are linearly related to the computed $\langle\alpha\rangle$ values with excellent statistics (r^2 = 0.99) as shown in Figure 4. An analogue $\langle\alpha\rangle$ vs V linear relationship has been recently established for α-helix oligoglycines.[41]

Polypeptides exhibit good transparency in the visible spectral region, absorbing near 6.5 eV.[13] This value is significantly lower than that for polyacetylene oligomers,[88] which are considered among the polymeric materials with the largest third-order NLO responses.[89−91] Thus, in order to add knowledge of the electronic structure of the investigated oligoglycines, we computed vertical electronic transitions to singlet excited states on the geometries of the neutral ground states. To this purpose, we used the configuration interaction singles (CIS) method[92] with the 6-31+G* basis set. Usually CIS computations overestimate experimental and high-level theoretical excitation energies;[92−96] nevertheless, they can be employed for

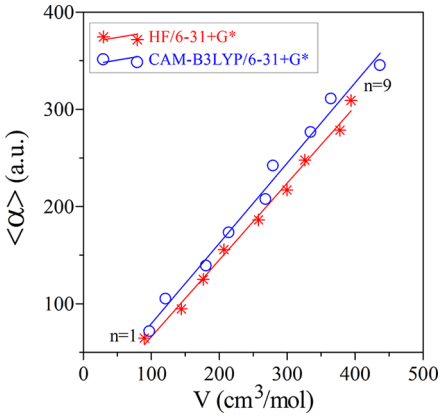

Figure 4. Relationship between the electronic average polarizability and molar volume (V) of the $H_2N-(CH_2-CO-NH)_n-CH_2COOH$ (n = 1–9) oligomers. HF/6-31+G*: $\langle\alpha\rangle = -13.167 + 0.791 \times V$ (r^2 = 0.99). CAM-B3LYP/6-31+G*: $\langle\alpha\rangle = -3.101 + 0.826 \times V$ (r^2 = 0.99).

qualitative interpretations. In Table 2, we collected the CIS/6-31+G* energy difference between the ground and the lowest-

Table 2. Vertical Transition Energy, E^{eg} (eV), Dipole Transition Moment, M_i^{eg} (au), and Oscillator Strength f (au) of the Lowest-Energy Dipole-Allowed Excited State of β-Strand Oligoglycines $H_2N-(CH_2-CO-NH)_n-CH_2COOH$ (n = 1–9)[a]

n	E^{eg}	M_i^{eg}	f
1	8.62	−0.83	0.22
2	8.56	1.04	0.23
3	8.52	1.46	0.46
4	8.49	1.95	0.79
5	8.47	2.27	1.07
6	8.46	2.55	1.34
7	8.45	2.79	1.61
8	8.44	−3.01	1.87
9	8.43	−3.21	2.12

[a]Calculations were carried out at the CIS/6-31+G* level.

energy dipole-allowed electronic excited state (E^{eg}), the corresponding i-component of the transition moment (M_i^{eg}), and the oscillator strength (f). The investigated peptides show a relatively intense absorption located at 8.4–8.6 eV. In particular, for the largest oligomers (n = 5–9), the E^{eg} value remains almost unvaried (within 0.04 eV). This transition involves a $\pi-\pi^*$ excitation mainly localized on vicinal peptidic C═O and N–H groups. It is consistent with the strong absorption for N-acetylglycine denoted as the NV_1 band and placed experimentally at 6.6[97] and 6.76 eV by CASPT2 computations.[98] For $H_2N-(CH_2-CO-NH)-CH_2COOH$, present CIS/6-31+G* calculations locate this transition at 8.62 eV with an f value of 0.22 au, which compares well with both the observed (0.22 au)[97] and CASPT2 (0.29 au)[98] data. The evolution of the electronic spectra along the chain length (n = 1–9) is displayed in Figure 5, which also includes the molecular orbital densities contributing to the NV_1 transition. As can be appreciated from Figure 5, at variance from the E^{eg} data, the intensity of the NV_1 transition is significantly affected by the chain length, regularly increasing with the increase of the n value. In particular, on passing from $H_2N-(CH_2-CO-NH)-CH_2COOH$ to $H_2N-(CH_2-CO-NH)_9-CH_2COOH$,

dx.doi.org/10.1021/jp403155q | J. Phys. Chem. A 2013, 117, 5184–5194

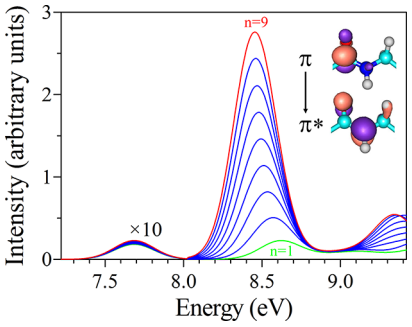

Figure 5. Simulated electronic absorption spectra of the $H_2N-(CH_2-CO-NH)_n-CH_2COOH$ (n = 1−9) oligomers. CIS/6- 31+G* results.

the $(M_i^{eg})^2$ value enhances by an order of magnitude, in line with the increase of the computed α_{zz} and $\langle\alpha\rangle$ values. Electronic polarizabilities can be calculated through the perturbation theory using the sum-over state (SOS) formulation[99,100]

$$\alpha_{ii} = 2\sum \frac{(M_i^{eg})^2}{E^{eg}} \quad (5)$$

In the presence of low-energy dipole-allowed electronic transitions, the SOS expression can be restricted to a few main contributing excited states. For all the investigated oligoglycines, the largest α_{zz} component is principally associated to the strong NV_1 electronic transition. Thus, assuming the two-state model,[100] we find a linear relationship between the calculated α_{zz} and $(M_i^{eg})^2$ values with excellent statistics (r^2 = 0.99). This relationship is illustrated in Figure 6.

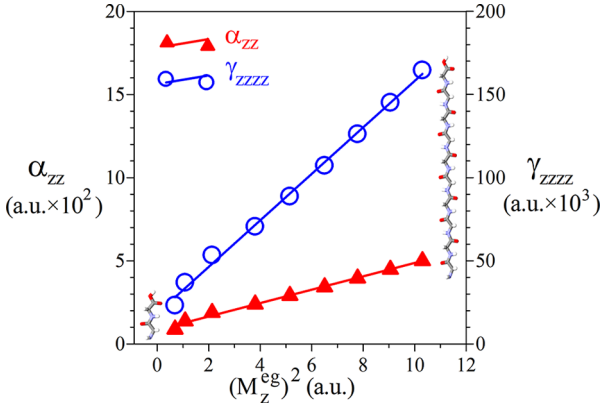

Figure 6. Relationships between the CAM-B3LYP/6-31+G* longitudinal (hyper)polarizabilities and CIS/6-31+G*$(M_i^{eg})^2$ values for the NV1 electronic transition of the $H_2N-(CH_2-CO-NH)_n-CH_2COOH$ (n = 1−9) oligomers. α_{zz} = 0.847 + 0.402 × $(M_i^{eg})^2$ (r^2 = 0.99); γ_{zzzz} = 18.439 + 13.974 × $(M_i^{eg})^2$ (r^2 = 1.00).

The above results indicate that the longitudinal polarizability (and also $\langle\alpha\rangle$) of the β-strand polyglycines is mainly ruled by the intensity of the strong low-energy dipole-allowed NV_1 excitation, the E^{eg} term being unimportant.

C. Second-Order Hyperpolarizabilities. Table 1 lists the longitudinal and average second-order hyperpolarizabilities of the investigated oligoglycines. As for the calculated α_{zz} values, γ_{zzzz} is the largest hyperpolarizability component, which for $H_2N-(CH_2-CO-NH)_9-CH_2-COOH$ at the HF/6-31+G* and CAM-B3LYP/6-31+G* levels recovers ca. 60% of the total second-order hyperpolarizability (γ_{xxxx} + γ_{yyyy} + γ_{zzzz} + 2γ_{xxyy} + 2γ_{xxzz} + 2γ_{yyzz}). Consistently with the calculated polarizabilities, the CCSD(T) electron correlation effects are positive but much more pronounced, enhancing the HF/6-31+G* γ_{zzzz} value of $H_2N-(CH_2-CO-NH)-CH_2COOH$ by 13 289 au (+105%), whereas the conventional B3LYP functional seriously overestimates the CCSD(T) γ_{zzzz} datum by 14 028 au (+54%). Differently, the MP2, CAM-B3LYP, and ωB97X-D levels provide a substantial improvement with respect to the B3LYP method, reproducing the CCSD(T)/6-31+G* γ_{zzzz} datum of $H_2N-(CH_2-CO-NH)-CH_2COOH$ by 2308 (−8.9%), 316 (+1.2%), and 1092 au (−4.2%), respectively. For the largest oligomers, we compared the performances of the employed levels by adopting the MP2 theory as the reference method. As for $H_2N-(CH_2-CO-NH)-CH_2COOH$, the effects of the electron correlation (HF → MP2) are positive also for the oligoglycines with $n \geq 2$, increasing the HF/6-31+G* γ_{zzzz} values by 70−80%. The CAM-B3LYP and ωB97X-D functionals show γ_{zzzz} values close to each other, giving reasonable results when compared to the MP2/6-31+G* data with percentage deviations up to 15%. The effects of basis sets here evaluated at the HF level show that the 6-31G basis set underestimates the γ_{zzzz} and $\langle\gamma\rangle$ values obtained with the 6-31+G* basis set by 16−42% and 42−61%, respectively, being significantly larger than the those for the calculated polarizabilities. However, in agreement with previous studies on polymeric systems,[101,102] the basis set effects are noticeably dependent on the molecular size; the larger the peptide chain, the smaller, the hyperpolarizability difference between the basis sets. The further augmentations of the basis set (6-31+G* → 6-31++G** and 6-31++G** → aug-cc-pVDZ) produce marginal or modest variations, increasing the γ_{zzzz} and $\langle\gamma\rangle$ values within 1−6% and 1−10%, respectively.

Like the computed μ and α data, the calculated γ_{zzzz} and $\langle\gamma\rangle$ values progressively rise with the increase of the n value. Specifically when considering the CAM-B3LYP/6-31+G* level of the calculation, the $\langle\gamma\rangle$ values vary between 11 408 au for the oligomer with n = 1 to 64 336 au for the oligomer with n = 9, while the γ_{zzzz} values range from 26 265 au (n = 1) to 189 335 au (n = 9). Figure 7 displays the evolutions of the γ_{zzzz} data per unit cell with the number of glycine units. By analogy to the $\Delta\alpha_{zz}$ and $\Delta\langle\alpha\rangle$ data, we evaluated the $\Delta\gamma_{zzzz}$ = $[\gamma_{zzzz}(n) - \gamma_{zzzz}(n-2)]/2$ and $\Delta\langle\gamma\rangle$ = $[\langle\gamma\rangle(n) - \langle\gamma\rangle(n-2)]/2$ properties

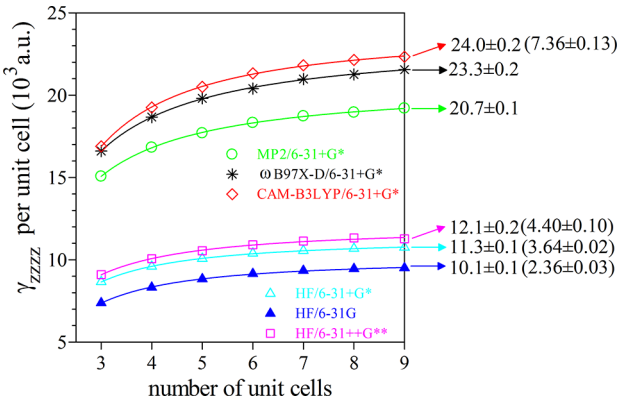

Figure 7. Calculated γ_{zzzz} per unit cell {γ_{zzzz} = $[\gamma_{zzzz}(n) - \gamma_{zzzz}(n-2)]/2$} of the $H_2N-(CH_2-CO-NH)_n-CH_2COOH$ (n = 1−9) oligomers as a function of the chain length. The reported data refer to the extrapolated properties in the limit of the polymer $\gamma_{zzzz}(n \to \infty)$. The value in parentheses refers to the $\Delta\langle\gamma\rangle(n \to \infty)$ datum.

dx.doi.org/10.1021/jp403155q | J. Phys. Chem. A 2013, 117, 5184−5194

in the limit of the polymer [$\Delta\gamma_{zzzz}(n \rightarrow \infty)$ and $\Delta\langle\gamma\rangle(n \rightarrow \infty)$], by using extrapolation fitting expressions similar to eq 4. The results for the $\Delta\gamma_{zzzz}(n \rightarrow \infty)$ values are inserted in Figure 7. Both the CAM-B3LYP and ωB97X-D functionals give reasonable estimates, overestimating the MP2/6-31+G* $\Delta\gamma_{zzzz}(n \rightarrow \infty)$ value by 2.6−3.3 × 10^3 au (13−16%). The effects of the basis sets on the $\Delta\gamma_{zzzz}(n \rightarrow \infty)$ values are rather modest, being ca. +12% and +7% for the 6-31G → 6-31+G* and 6-31+G* → 6-31++G** switching, respectively. When we consider the CAM-B3LYP/6-31+G* (HF/6-31+G*) average hyperpolarizabilities, the extrapolated $\Delta\langle\gamma\rangle$ value in the limit of the polyglycine is 7.36 ± 0.13 × 10^3 au (3.64 ± 0.02 × 10^3 au). Note that the $\Delta\gamma_{zzzz}$ and $\Delta\langle\gamma\rangle$ data for the longest oligoglycine nearly reach the saturation toward the asymptotic values of the polymer (within 1−5%), whereas the $\Delta\gamma_{zzzz}(n \rightarrow \infty)/[5\Delta\langle\gamma\rangle(n \rightarrow \infty)]$ ratio is almost unaffected by the level of calculation amounting to 0.62 for HF/6-31+G* and 0.65 for CAM-B3LYP/6-31+G*.

Similarly to the electronic polarizabilities, the second-order hyperpolarizabilities of the β-strand oligoglycines can be described by the two-state approximation, the γ_{zzzz} values (n = 1−9) being linearly related to the calculated CIS/6-31+G* $(M_i^{eg})^2$ data of the NV_1 electronic transition. The linear γ_{zzzz} vs $(M_i^{eg})^2$ relationship is illustrated in Figure 6, showing satisfactory statistics (r^2 = 1.00). As a consequence, good linear relationships between γ_{zzzz} and α_{zz} values (and also between $\langle\gamma\rangle$ and $\langle\alpha\rangle$ values) are established (Figure 8), by analogy to those recently found for α-helix oligoglycines,[41] nucleic acid bases,[58] and aliphatic amino acids.[103,104]

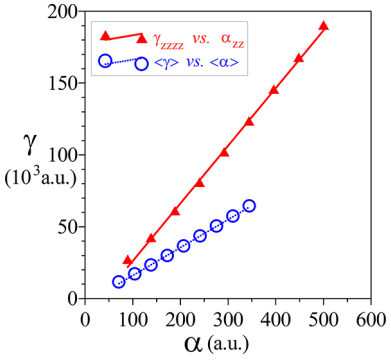

Figure 8. Relationships between the static electronic polarizabilities and second-order hyperpolarizabilities of the $H_2N-(CH_2-CO-NH)_n-CH_2COOH$ (n = 1−9) oligomers. CAM-B3LYP/6-31+G* results. γ_{zzzz} = −14.007 + 0.401 × α_{zz} (r^2 = 1.00); $\langle\gamma\rangle$ = −3.426 + 0.195 × $\langle\alpha\rangle$ (r^2 = 1.00).

For the largest oligomer, we investigated the individual atomic contribution to the longitudinal second-order hyperpolarizability, calculating electric field-induced polarization effects. Specifically, to obtain electric field-induced charge transfer for the ith atom A_i [$\delta q_z(A_i)$], we used an expression analogue to that previously reported for spatial γ density analysis:[105−107] $\delta q_z(A_i) = \{q(A_i, 2F_z) - q(A_i, -2F_z) - 2[q(A_i, F_z) - q(A_i, -F_z)]\}/2(F_z)^3$, where $q(A_i, F_z)$ is the charge on the ith atom A_i in the presence of an external electric field F_z applied along the z-axis direction. A similar approach has been previously adopted to characterize the atomic contributions to the calculated electronic polarizabilities of Si_n[108] and Al_nP_n clusters.[109] The atomic charges were here computed at the CAM-B3LYP/6-31+G* level using the Merz−Singh−Kollman population analysis.[110,111] For a certain pair of vicinal positive and negative $\delta q_z(A_i)$ contributions, the sign is positive if the positive-to-negative $\delta q_z(A_i)$ direction coincides with the positive direction of the coordinate frame. Figure 9 displays

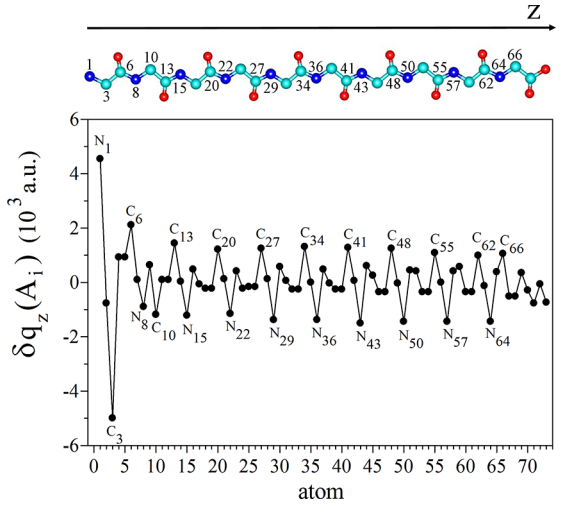

Figure 9. Electric field induced atomic charge transfers [$\delta q_z(A_i)$] for the $H_2N-(CH_2-CO-NH)_9-CH_2COOH$ oligomer. CAM-B3LYP/6-31+G* results. Colors: cyan (carbon), blue (nitrogen), and red (oxygen).

the $\delta q_z(A_i)$ data for $H_2N-(CH_2-CO-NH)_9-CH_2COOH$. As can be appreciated from the Figure, the largest negative $\delta q_z(A_i)$ values are principally kept by the nitrogen atoms, with the notable exception of the N_1 atom. Differently, the carbon atoms of the C=O groups hold the greatest positive $\delta q_z(A_i)$ values. The largest positive-to-negative $\delta q_z(A_i)$ couple is given by the bonded N_1 and C_3 atoms. In addition, all the peptide C−N bonds furnish similar positive-to-negative $\delta q_z(A_i)$ pairs, concordantly contributing together with the N_1-C_3 bond to the positive and relatively large magnitude of the γ_{zzzz} component.

D. Effect of the Conformation: Comparison between β-Strands and α-Helices. In a recent study, we have performed CAM-B3LYP/6-31+G* computations on the μ, α, and γ properties of single chain α-helix oligoglycines (n = 1−9),[41] which can be compared to the present results obtained for the β-strands. Except for the smallest oligomer, the α-helices are predicted to be significantly more polar than the β-strands, in agreement with the B3LYP/6-31G* data previously reported by Wu and Zhao.[37] In particular for the largest peptide, the CAM-B3LYP/6-31+G* $\mu(\alpha\text{-helix})/\mu(\beta\text{-strand})$ ratio is calculated to be 1.7, which agrees well with the ratio of 1.8 obtained by the B3LYP/6-31G* values.[37] The α-helix/β-strand μ differences are mainly attributed to the presence of the intramolecular hydrogen bonds in the α-helices, which exalt the cooperativity of the glycine units and enhance the almost parallel $\mu_{C=O}$ and μ_{H-N} bond dipole moments. A rather different behavior occurs for the β-strands, where the neighbor $\mu_{C=O}$ contributions are almost antiparallel to each other (a similar situation exists also for the μ_{H-N} contributions), resulting in a partial cancellation effect. In the case of the electronic polarizabilities, for the oligomer with n = 1 the $\alpha_{zz}(\beta\text{-strand})/\alpha_{zz}(\alpha\text{-helix})$ and $\langle\alpha\rangle(\beta\text{-strand})/\langle\alpha\rangle(\alpha\text{-helix})$ ratios are near unity (1.09 and 1.01, respectively). For the largest peptide (n = 9), the corresponding ratios are greater, increasing to 1.22

dx.doi.org/10.1021/jp403155q | J. Phys. Chem. A 2013, 117, 5184−5194

and 1.04, respectively, in agreement with the molar volume ratios of 1.08. These results suggest that, when the peptide chain lengthens, the electron mobility in the β-strands rises more rapidly with respect to the α-helices. The above findings on the polarizabilities are also corroborated by the second-order hyperpolarizability data. For $H_2N-(CH_2-CO-NH)-CH_2COOH$, $\langle\gamma\rangle$ is little affected by the conformation, being 11 408 au for the β-strand and 11 900 au for the α-helix form. However, $\gamma_{zzzz}(\beta\text{-strand})$ is higher than $\gamma_{zzzz}(\alpha\text{-helix})$ by ca. 5300 au (+25%). As the number of glycine units increases, the differences steadily rise. Indeed, for $H_2N-(CH_2-CO-NH)_9-CH_2COOH$, the $\gamma_{zzzz}(\beta\text{-strand})/\gamma_{zzzz}(\alpha\text{-helix})$ and $\langle\gamma\rangle(\beta\text{-strand})/\langle\gamma\rangle(\alpha\text{-helix})$ ratios are predicted to be 2.26 and 1.09, respectively, in contrast to the results obtained for the μ values. These results, confirming the above trend for the computed polarizabilities, support an enhanced electron mobility when going from the α-helix to the β-strand polyglycines, which is especially magnified along the longitudinal direction. However, it is important noting that, when we compare the γ values for unit of length, the $\gamma_{zzzz}(\beta\text{-strand})/\gamma_{zzzz}(\alpha\text{-helix})$ ratios for $H_2N-(CH_2-CO-NH)_9-CH_2COOH$ reduces to ca. 1.

4. CONCLUSIONS

In this study, we have applied the HF, MP2, and DFT methods to investigate the evolution of dipole moments, static electronic polarizabilities, and second-order hyperpolarizabilities of $H_2N-(CH_2-CO-NH)_n-CH_2COOH$ (n = 1−9) single chain oligoglycines. All computations have been carried out in the gas phase for the β-strand conformation. A variety of basis sets such as 6-31G, 6-31+G*, 6-31++G**, and aug-cc-pVDZ have been used.

The electron correlation effects obtained at the MP2 level are rather modest for the dipole moments and polarizabilities, whereas positive and remarkable for the second-order hyperpolarizabilities, causing an increase of the HF data by ca. 70−80%. Both the long-range corrected CAM-B3LYP and ωB97X-D functionals provide good performances on the computed properties, nicely reproducing the MP2 and CCSD(T) data. The calculated (hyper)polarizabilities are dependent on the basis sets: the largest effects occur when passing from the 6-31G to 6-31+G* basis set; further basis set extension having a negligible or modest influence.

The evolutions of the (hyper)polarizabilities with the chain length have been elucidated through the two-state model applied to the typical strong $\pi-\pi^*$ NV_1 electronic transition mainly localized on the −NH−CO− peptide moieties. Interesting linear relationships have been established between the longitudinal (hyper)polarizabilities and the square of the transition moment of the NV_1 excitation. The longitudinal and average electric properties per unit cell have been examined as a function of the number of glycine units, estimating the values in the limit of the polymer. For the largest oligoglycine, the sign and magnitude of the longitudinal second-order hyperpolarizability component have been rationalized on the basis of electric field induced atomic charge polarizations involving the peptide C−N bonds. The electric properties here computed for the β-strand forms have been compared to the results recently obtained for the α-helices obtained at the same level of theory. The calculated polarizabilities are not affected in any significant way by the structure. Differently, when going from the α-helices to the β-strands, the second-order hyperpolarizabilities remarkably increase, in contrast to their relative dipole moments for which $\mu(\beta\text{-strand}) < \mu(\alpha\text{-helix})$.

AUTHOR INFORMATION

Corresponding Author

* Phone: 0039-95-7385008. E-mail: agalparone@unict.it.

Notes

The authors declare no competing financial interest.

REFERENCES

(1) Chemla, D. S., Zyss, J., Eds. *Nonlinear Optical Properties of Organic Molecules and Crystals*; Academic Press: San Diego, CA, 1987; Vols. *1 and 2*.

(2) Prasad, P. N.; Williams, D. J. *Introduction to Nonlinear Optical Effects in Molecules and Polymers*; J. Wiley & Sons, Inc.: New York, 1991.

(3) Burland, D. M.; Miller, R. D.; Walsh, C. A. Second-Order Nonlinearity in Poled-Polymer Systems. *Chem. Rev.* **1994**, *94*, 31−75.

(4) Moerner, W. E.; Silence, S. M. Polymeric Photorefractive Materials. *Chem. Rev.* **1994**, *94*, 127−155.

(5) Xu, T.; Wu, S. P.; Miloradovic, I.; Therien, M. J.; Blasie, J. K. Incorporation of Designed Extended Chromophores into Amphiphilic 4-Helix Bundle Peptides for Nonlinear Optical Biomolecular Materials. *Nano Lett.* **2006**, *6*, 2387−2394.

(6) Bautista, E. J.; Yan, L.; Seminario, J. M. Ab Initio Analysis of Electron Transport in Oligoglycines. *J. Phys. Chem. C* **2007**, *111*, 14552−14559.

(7) Cristancho, D.; Seminario, J. M. Polypeptides in Alpha-Helix Conformation Perform as Diodes. *J. Chem. Phys.* **2010**, *132*, 065102.

(8) Takashima, S. The Structure and Dipole Moment of Globular Proteins in Solution and Crystalline States: Use of NMR and X-ray Databases for the Numerical Calculation of Dipole Moment. *Biopolymers* **2001**, *58*, 398−409.

(9) Antoine, R.; Compagnon, I.; Rayane, D.; Broyer, M.; Dugourd, P.; Breaux, G.; Hagemeister, F. C.; Pippen, D.; Hudgins, R. R.; Jarrold, M. F. Electric Dipole Moments and Conformations of Isolated Peptides. *Eur. Phys. J. D* **2002**, *20*, 583−587.

(10) Shimizu, K.; Chaimovich, H.; Farah, J. P. S.; Dias, L. G.; Bostick, D. L. Calculation of the Dipole Moment for Polypeptides Using the Generalized Born-Electronegativity Equalization Method: Results in Vacuum and Continuum-Dielectric Solvent. *J. Phys. Chem. B* **2004**, *108*, 4171−4177.

(11) Rogers, S. S.; Venema, P.; van der Ploeg, J. P. M.; van der Linden, E.; Sagis, L. M. C.; Donald, A. M. Investigating the Permanent Electric Dipole Moment of β-Lactoglobulin Fibrils, Using Transient Electric Birefringence. *Biopolymers* **2006**, *82*, 241−252.

(12) Miller, C. A.; Hernández-Ortiz, J. P.; Abbott, N. L.; Gellman, S. H.; de Pablo, J. J. Dipole-Induced Self-Assembly of Helical β-Peptides. *J. Chem. Phys.* **2008**, *129*, 015102.

(13) Robin, M. B. *Higher Excited States of Polyatomic Molecules*; Academic Press: New York, 1975, Vol. *2*.

(14) Burland, D. M.; Rice, J. E.; Downing, J.; Michl, J. Design of Chromophores for Nonlinear Optical Applications. *Proc. SPIE-Int. Soc. Opt. Eng.* **1991**, *1560*, 111−119.

(15) Burland, D. M.; Miller, R. D.; Reiser, O.; Twieg, R. J.; Walsh, C. A. The Design, Synthesis, and Evaluation of Chromophores for Second-Harmonic Generation in a Polymer Waveguide. *J. Appl. Phys.* **1992**, *71*, 410−417.

(16) Salafsky, J. S. Second-Harmonic Generation as a Probe of Conformational Change in Molecules. *Chem. Phys. Lett.* **2003**, *381*, 705−709.

(17) Sliwa, M.; Nakatani, K.; Asahi, T.; Lacroix, P. G.; Pansu, R. B.; Masuhara, H. Polarization and Wavelength Dependent Nonlinear Optical Properties of a Photo-Switchable Organic Crystal. *Chem. Phys. Lett.* **2007**, *437*, 212−217.

(18) Perrenoud-Rinuy, J.; Brevet, P.-F.; Girault, H. H. Second Harmonic Generation Study of Myoglobin and Hemoglobin and Their Protoporphyrin IX Chromophore at the Water/1,2-Dichloroethane Interface. *Phys. Chem. Chem. Phys.* **2002**, *4*, 4774−4781.

(19) Mitchell, S. A.; McAloney, R. A. Second Harmonic Optical Activity of Tryptophan Derivatives Adsorbed at the Air/Water Interface. *J. Phys. Chem. B* **2004**, *108*, 1020−1029.
(20) Salafsky, J. S. Second-Harmonic Generation for Studying Structural Motion of Biological Molecules in Real Time and Space. *Phys. Chem. Chem. Phys.* **2007**, *9*, 5704−5711.
(21) Williams, R. M.; Zipfel, W. R.; Webb, W. W. Interpreting Second-Harmonic Generation Images of Collagen I Fibrils. *Biophys. J.* **2005**, *88*, 1377−1386.
(22) Chen, W.-L.; Li, T.-H.; Su, P.-J.; Chou, C.-K.; Fwu, P. T.; Lin, S.-J.; Kim, D.; So, P. T. C.; Dong, C.-Y. Second Harmonic Generation χ Tensor Microscopy for Tissue Imaging. *Appl. Phys. Lett.* **2009**, *94*, 183902/1−3.
(23) Salafsky, J. S.; Cohen, B. A Second-Harmonic-Active Unnatural Amino Acid as a Structural Probe of Biomolecules on Surfaces. *J. Phys. Chem. B* **2008**, *112*, 15103−15107.
(24) Antoine, R.; Compagnon, I.; Rayane, D.; Broyer, M.; Dugourd, P.; Breaux, G.; Hagemeister, F. C.; Pippen, D.; Hudgins, R. R.; Jarrold, M. F. Electric Susceptibility of Unsolvated Glycine-Based Peptides. *J. Am. Chem. Soc.* **2002**, *124*, 6737−6741.
(25) Antoine, R.; Broyer, M.; Dugourd, P.; Breaux, G.; Hagemeister, F. C.; Pippen, D.; Hudgins, R. R.; Jarrold, M. F. Direct Probing of Zwitterion Formation in Unsolvated Peptides. *J. Am. Chem. Soc.* **2003**, *125*, 8996−8997.
(26) Duboisset, J.; Matar, G.; Russier-Antoine, I.; Benichou, E.; Bachelier, G.; Jonin, C.; Ficheux, D.; Besson, F.; Brevet, P. F. First Hyperpolarizability of the Natural Aromatic Amino Acids Tryptophan, Tyrosine, and Phenylalanine and the Tripeptide Lysine-Tryptophan-Lysine Determined by Hyper-Rayleigh Scattering. *J. Phys. Chem. B.* **2010**, *114*, 13861−13865.
(27) Perry, J. M.; Moad, A. J.; Begue, N. J.; Wampler, R. D.; Simpson, G. J. Electronic and Vibrational Second-Order Nonlinear Optical Properties of Protein Secondary Structural Motifs. *J. Phys. Chem. B* **2005**, *109*, 20009−20026.
(28) Mitchell, S. A.; McAloney, R. A.; Moffatt, D.; Mora-Diez, N.; Zgierski, M. Z. Second-Harmonic Generation Optical Activity of a Polypeptide α-Helix at the Air/Water Interface. *J. Chem. Phys.* **2005**, *122*, 114707.
(29) Gualtieri, E. J.; Haupert, L. M.; Simpson, G. J. Interpreting Nonlinear Optics of Biopolymer Assemblies: Finding a Hook. *Chem. Phys. Lett.* **2008**, *465*, 167−174.
(30) Loison, C.; Simon, D. Additive Model for the Second Harmonic Generation Hyperpolarizability Applied to a Collagen-Mimicking Peptide $(Pro\text{-}Pro\text{-}Gly)_{10}$. *J. Phys. Chem. A* **2010**, *114*, 7769−7779.
(31) Tuer, A. E.; Krouglov, S.; Prent, N.; Cisek, R.; Sandkuijl, D.; Yasufuku, K.; Wilson, B. C.; Barzda, V. Nonlinear Optical Properties of Type I Collagen Fibers Studied by Polarization Dependent Second Harmonic Generation Microscopy. *J. Phys. Chem. B* **2011**, *115*, 12759−12769.
(32) Lotz, B. Crystal Structure of Polyglycine I. *J. Mol. Biol.* **1974**, *87*, 169−180.
(33) Crick, F. H. C.; Rich, A. Structure of Polyglycine II. *Nature* **1955**, *176*, 780−781.
(34) Scheiner, S.; Kern, C. W. Energies of Polypeptides: Theoretical Conformational Study of Polyglycine Using Quantum Mechanical Partitioning. *Proc. Natl. Acad. Sci. U.S.A.* **1978**, *75*, 2071−2075.
(35) Improta, R.; Barone, V.; Kudin, K. N.; Scuseria, G. E. Structure and Conformational Behavior of Biopolymers by Density Functional Calculations Employing Periodic Boundary Conditions. I. The Case of Polyglycine, Polyalanine, and Poly-α-aminoisobutyric Acid in Vacuo. *J. Am. Chem. Soc.* **2001**, *123*, 3311−3322.
(36) Wieczorek, R.; Dannenberg, J. J. Hydrogen-Bond Cooperativity, Vibrational Coupling, and Dependence of Helix Stability on Changes in Amino Acid Sequence in Small 3_{10}-Helical Peptides. A Density Functional Theory Study. *J. Am. Chem. Soc.* **2003**, *125*, 14065−14071.
(37) Wu, Y.-D.; Zhao, Y.-L. A Theoretical Study on the Origin of Cooperativity in the Formation of 3_{10}- and α-Helices. *J. Am. Chem. Soc.* **2001**, *123*, 5313−5319.
(38) Horváth, V.; Varga, Z.; Kovács, A. Long-Range Effects in Oligopeptides. A Theoretical Study of the β-Sheet Structure of Gly_n (n = 2−10). *J. Phys. Chem. A* **2004**, *108*, 6869−6873.
(39) Chaudhuri, P.; Canuto, S. Rayleigh Scattering Properties of Small Polyglycine molecule. *J. Mol. Struct.* **2006**, *760*, 15−20.
(40) Alparone, A. Ionization Energy and Electron Affinity of Oligoglycines: a CAM-B3LYP Density Functional Theory Study. *Monatsh. Chem.* **2012**, *143*, 513−517.
(41) Alparone, A. Response Electric Properties of α-Helix Polyglycines: a CAM-B3LYP DFT Investigation. *Chem. Phys. Lett.* **2013**, *563*, 88−92.
(42) Champagne, B.; Perpete, E. A.; van Gisbergen, S. J. A.; Baerends, E.-J.; Snijders, J. G.; Soubra-Ghaoui, C.; Robins, K. A.; Kirtman, B. Assessment of Conventional Density Functional Schemes for Computing the Polarizabilities and Hyperpolarizabilities of Conjugated Oligomers: An ab Initio Investigation of Polyacetylene Chains. *J. Chem. Phys.* **1998**, *109*, 10489−10498.
(43) Sekino, H.; Maeda, Y.; Kamiya, M.; Hirao, K. Polarizability and Second Hyperpolarizability Evaluation of Long Molecules by the Density Functional Theory with Long-Range Correction. *J. Chem. Phys.* **2007**, *126*, 014107.
(44) Kirtman, B.; Bonness, S.; Ramirez-Solis, A.; Champagne, B.; Matsumoto, H.; Sekino, H. Calculation of Electric Dipole (Hyper)-polarizabilities by Long-Range-Correction Scheme in Density Functional Theory: A Systematic Assessment for Polydiacetylene and Polybutatriene Oligomers. *J. Chem. Phys.* **2008**, *128*, 114108.
(45) Song, J.-W.; Watson, M. A.; Sekino, H.; Hirao, K. Nonlinear Optical Property Calculations of Polyynes with Long-Range Corrected Hybrid Exchange-Correlation Functional. *J. Chem. Phys.* **2008**, *129*, 024117−.
(46) Loboda, O.; Zalesny, R.; Avramopoulos, A.; Luis, J.-M.; Kirtman, B.; Tagmatarchis, N.; Reis, H.; Papadopoulos, M. G. Linear and Nonlinear Optical Properties of [60]Fullerene Derivatives. *J. Phys. Chem. A* **2009**, *113*, 1159−1170.
(47) Limacher, P. A.; Li, Q.; Lüthi, H. P. On the Effect of Electron Correlation on the Static Second Hyperpolarizability of π Conjugated Oligomer Chains. *J. Chem. Phys.* **2011**, *135*, 014111.
(48) Ferrighi, L.; Frediani, L.; Cappelli, C.; Salek, P.; Agren, H.; Helgaker, T.; Ruud, K. Density-Functional-Theory Study of the Electric-Field-Induced Second Harmonic Generation (EFISHG) of Push-Pull Phenylpolyenes in Solution. *Chem. Phys. Lett.* **2006**, *425*, 267−272.
(49) Jacquemin, D.; Perpète, E. A.; Scalmani, G.; Frisch, M. J.; Kobayashi, R.; Adamo, C. Assessment of the Efficiency of Long-Range Corrected Functionals for Some Properties of Large Compounds. *J. Chem. Phys.* **2007**, *126*, 144105.
(50) Pluta, T.; Kolaski, M.; Medved, M.; Budzák, S. Dipole Moment and Polarizability of the Low-Lying Excited States of Uracil. *Chem. Phys. Lett.* **2012**, *546*, 24−29.
(51) Alparone, A. Structural, Energetic and Response Electric Properties of Cyclic Selenium Clusters: An Ab Initio and Density Functional Theory Study. *Theor. Chem. Acc.* **2012**, *131*, 1239−.
(52) Alipour, M.; Mohajeri, A. Assessing the Performance of Density Functional Theory for the Dynamic Polarizabilities of Amino Acids: Treatment of Correlation and Role of Exact Exchange. *Int. J. Quantum Chem.* **2013**, *113*, 1803−1811.
(53) Medved, M.; Budzák, S.; Pluta, T. Static NLO Responses of Fluorinated Polyacetylene Chains Evaluated with Long-Range Corrected Density Functionals. *Chem. Phys. Lett.* **2011**, *515*, 78−84.
(54) Jacquemin, D.; Perpète, E. A.; Ciofini, I.; Adamo, C. Revisiting the Relationship between the Bond Length Alternation and the First Hyperpolarizability with Range-Separated Hybrid Functionals. *J. Comput. Chem.* **2008**, *29*, 921−925.
(55) Borini, S.; Limacher, P. A.; Lüthi, H. P. A Systematic Analysis of the Structure and (Hyper)polarizability of Donor−Acceptor Substituted Polyacetylenes Using a Coulomb-Attenuating Density Functional. *J. Chem. Phys.* **2009**, *131*, 124105.

(56) Alparone, A. Comparative Study of CCSD(T) and DFT Methods: Electronic (Hyper)polarizabilities of Glycine. *Chem. Phys. Lett.* **2011**, *514*, 21−25.
(57) Limacher, P. A.; Mikkelsen, K. V.; Lüthi, H. P. On the Accurate Calculation of Polarizabilities and Second Hyperpolarizabilities of Polyacetylene Oligomer Chains using the CAM-B3LYP Density Functional. *J. Chem. Phys.* **2009**, *130*, 194114.
(58) Alparone, A. Linear and Nonlinear Optical Properties of Nucleic Acid Bases. *Chem. Phys.* **2013**, *410*, 90−98.
(59) Frisch, M. J.; Trucks, G. W.; Schlegel, H. B.; Scuseria, G. E.; Robb, M. A.; Cheeseman, J. R.; Scalmani, G.; Barone, V.; Mennucci, B.; Petersson, G. A.; et al. *Gaussian 09*, revision A.02; Gaussian, Inc.: Wallingford, CT, 2009.
(60) Schmidt, M. W.; Baldridge, K. K.; Boatz, J. A.; Elbert, S. T.; Gordon, M. S.; Jensen, J. H.; Koseki, S.; Matsunaga, N.; Nguyen, K. A.; Su, S.; et al. General Atomic and Molecular Electronic Structure System. *J. Comput. Chem.* **1993**, *14*, 1347−1363.
(61) Sekino, H.; Bartlett, R. J. Frequency Dependent Nonlinear Optical Properties of Molecules. *J. Chem. Phys.* **1986**, *85*, 976−989.
(62) Karna, S. P.; Dupuis, M. Frequency Dependent Nonlinear Optical Properties of Molecules: Formulation and Implementation in the HONDO Program. *J. Comput. Chem.* **1991**, *12*, 487−504.
(63) Shelton, D. P.; Rice, J. E. Measurements and Calculations of the Hyperpolarizabilities of Atoms and Small Molecules in the Gas Phase. *Chem. Rev.* **1994**, *94*, 3−29.
(64) Rice, J. E.; Amos, R. D.; Colwell, S. M.; Handy, N. C.; Sanz, J. Frequency Dependent Hyperpolarizabilities with Application to Formaldehyde and Methyl Fluoride. *J. Chem. Phys.* **1990**, *93*, 8828−8839.
(65) Sekino, H.; Bartlett, R. J. Molecular Hyperpolarizabilities. *J. Chem. Phys.* **1993**, *98*, 3022−3037.
(66) Sim, F.; Chin, S.; Dupuis, M.; Rice, J. E. Electron Correlation Effects in Hyperpolarizabilities of *p*-Nitroaniline. *J. Phys. Chem.* **1993**, *97*, 1158−1163.
(67) Maroulis, G.; Thakkar, A. J. Polarizabilities and Hyperpolarizabilities of F_2. *J. Chem. Phys.* **1989**, *90*, 366−370.
(68) Archibong, E. F.; Thakkar, A. J. Hyperpolarizabilities and Polarizabilities of Li^{-1} and B^{+}: Finite-Field Coupled-Cluster Calculations. *Chem. Phys. Lett.* **1990**, *173*, 579−584.
(69) Archibong, E. F.; Thakkar, A. J. Static Polarizabilities and Hyperpolarizabilities, and Multipole Moments for Cl_2 and Br_2. Electron Correlation and Molecular Vibration Effects. *Chem. Phys. Lett.* **1993**, *201*, 485−492.
(70) Champagne, B.; Vanderhoeven, H.; Perpète, E. A.; André, J.-M. Curvature versus Nuclear Relaxation Contributions to the Static Vibrational Polarizability of Polyacetylene Chains. *Chem. Phys. Lett.* **1996**, *248*, 301−308.
(71) Champagne, B.; Mosley, D. H. Electron Correlation Effects on the Static Longitudinal Second Hyperpolarizability of Polymeric Chains. Møller−Plesset Perturbation Theory Investigation of Hydrogen Model Chains. *J. Chem. Phys.* **1996**, *105*, 3592−3603.
(72) Becke, A. D. Density-Functional Thermochemistry. III. The Role of Exact Exchange. *J. Chem. Phys.* **1993**, *98*, 5648−5652.
(73) Lee, C.; Yang, A. D.; Parr, R. G. Development of the Colle−Salvetti Correlation-Energy Formula into a Functional of the Electron Density. *Phys. Rev. B* **1988**, *37*, 785−789.
(74) Yanai, T.; Tew, D.; Handy, N. C. A New Hybrid Exchange-Correlation Functional Using the Coulomb-Attenuating Method (CAM-B3LYP). *Chem. Phys. Lett.* **2004**, *393*, 51−57.
(75) Chai, J.-D.; Head-Gordon, M. Long-Range Corrected Hybrid Density Functionals with Damped Atom−Atom Dispersion Corrections. *Phys. Chem. Chem. Phys.* **2008**, *10*, 6615−6620.
(76) Maroulis, G. Hyperpolarizability of H_2O Revisited: Accurate Estimate of the Basis Set Limit and the Size of Electron Correlation Effects. *Chem. Phys. Lett.* **1998**, *289*, 403−411.
(77) Xenides, D.; Maroulis, G. Basis Set and Electron Correlation Effects on the First and Second Static Hyperpolarizability of SO_2. *Chem. Phys. Lett.* **2000**, *319*, 618−624.
(78) Bishop, D. M.; Maroulis, G. Accurate Prediction of Static Polarizabilities and Hyperpolarizabilities. A Study on FH ($X^1\Sigma^+$). *J. Chem. Phys.* **1985**, *82*, 2380−291.
(79) Rice, J. E.; Handy, N. C. The Calculation of Frequency-Dependent Polarizabilities as Pseudo-Energy Derivatives. *J. Chem. Phys.* **1991**, *94*, 4959−4971.
(80) Torrent-Sucarrat, M.; Solà, M.; Duran, M.; Luis, J. M.; Kirtman, B. Basis Set and Electron Correlation Effects on ab Initio Electronic and Vibrational Nonlinear Optical Properties of Conjugated Organic Molecules. *J. Chem. Phys.* **2003**, *118*, 711−718.
(81) Librando, V.; Alparone, A.; Minniti, Z. Computational Study on Dipole Moment, Polarizability and Second Hyperpolarizability of Nitronaphthalenes. *J. Mol. Struct. (THEOCHEM)* **2008**, *856*, 105−111.
(82) Champagne, B.; Spassova, M. Theoretical Investigation on the Polarizability and Second Hyperpolarizability of Polysilole. *Chem. Phys. Lett.* **2009**, *471*, 111−115.
(83) Jacquemin, D.; André, J.-M.; Perpète, E. A. Geometry, Dipole Moment, Polarizability and First Hyperpolarizability of Polymethineimine: An Assessment of Electron Correlation Contributions. *J. Chem. Phys.* **2004**, *121*, 4389−4396.
(84) Jacquemin, D.; Perpète, E. A. Ab Initio Assessment of the First Hyperpolarizability of Saturated and Unsaturated Polyaminoborane/Polyphosphinoborane Copolymers. *J. Phys. Chem A* **2005**, *109*, 6380−6386.
(85) Kirtman, B. Convergence of Finite Chain Approximation for Linear and Non-Linear Polarizabilities of Polyacetylene. *Chem. Phys. Lett.* **1988**, *143*, 81−83.
(86) Toto, J. L.; Toto, T. T.; de Melo, C. P.; Robins, K. A. Abinitio Polarizability Study of Polypyrrole. *J. Chem. Phys.* **1995**, *102*, 8048−8052.
(87) Mochizuki, Y.; Ishikawa, T.; Tanaka, K.; Tokiwa, H.; Nakano, T.; Tanaka, S. Dynamic Polarizability Calculation with Fragment Molecular Orbital Scheme. *Chem. Phys. Lett.* **2006**, *418*, 418−422.
(88) D'Amico, K. L.; Manos, C.; Christensen, R. L. Electronic Energy Levels in a Homologous Series of Unsubstituted Linear Polyenes. *J. Am. Chem. Soc.* **1980**, *102*, 1777−1782.
(89) Sinclair, M.; Moses, D.; Heeger, A. J.; Vilhelmsson, K.; Valk, B.; Salour, M. Measurement of the Third Order Susceptibility of *trans*-Polyacetylene by Third Harmonic Generation. *Solid State Commun.* **1987**, *61*, 221−225.
(90) Heeger, A. J.; Moses, D.; Sinclair, M. Nonlinear Excitations and Nonlinear Phenomena in Conductive Polymers. *Synth. Met.* **1987**, *17*, 343−348.
(91) Kajzar, F.; Etemad, S.; Baker, G. L.; Messier, J. $\chi^{(3)}$ of *trans*-$(CH)_x$: Experimental Observation of $2A_g$ Excited State. *Synth. Met.* **1987**, *17*, 563−567.
(92) Foresman, J. B.; Head-Gordon, M.; Pople, J. A.; Frisch, M. J. Toward a Systematic Molecular Orbital Theory for Excited States. *J. Phys. Chem.* **1992**, *96*, 135−149.
(93) Hadad, C. M.; Foresman, J. B.; Wiberg, K. B. Excited States of Carbonyl Compounds. 1. Formaldehyde and Acetaldehyde. *J. Phys. Chem.* **1993**, *97*, 4293−4312.
(94) Jean, J. .M; Hall, K. B. Theoretical Study of the Excited State Properties and Transitions of 2-Aminopurine in the Gas Phase and in Solution. *J. Phys. Chem. A* **2000**, *104*, 1930−1937.
(95) Dreuw, A.; Fleming, G. R.; Head-Gordon, M. Chlorophyll Fluorescence Quenching by Xanthophylls. *Phys. Chem. Chem. Phys.* **2003**, *5*, 3247−3256.
(96) Jacquemin, D.; Perpète, E. A.; Assfeld, X.; Scalmani, G.; Frisch, M. J.; Adamo, C. The Geometries, Absorption and Fluorescence Wavelengths of Solvated Fluorescent Coumarins: A CIS and TD-DFT Comparative Study. *Chem. Phys. Lett.* **2007**, *438*, 208−212.
(97) Clark, L. B. Polarization Assignments in the Vacuum UV Spectra of the Primary Amide, Carboxyl, and Peptide Groups. *J. Am. Chem. Soc.* **1995**, *117*, 7974−7986.
(98) Serrano-Andrés, L.; Fulscher, M. P. Theoretical Study of the Electronic Spectroscopy of Peptides. 2. Glycine and *N*-Acetylglycine. *J. Am. Chem. Soc.* **1996**, *118*, 12200−12206.

(99) Orr, B. J.; Ward, J. F. Perturbation Theory of the Non-Linear Optical Polarization of an Isolated System. *Mol. Phys.* **1971**, *20*, 513−526.
(100) Meyers, F.; Marder, S. R.; Pierce, B. M.; Brédas, J.-L. Electric Field Modulated Nonlinear Optical Properties of Donor-Acceptor Polyenes: Sum-Over-States Investigation of the Relationship between Molecular Polarizabilities (α, β, and γ) and Bond Length Alternation. *J. Am. Chem. Soc.* **1994**, *116*, 10703−10714.
(101) Hurst, G. J. B.; Dupuis, M.; Clementi, E. Ab Initio Analytic Polarizability, First and Second Hyperpolarizabilities of Large Conjugated Organic Molecules: Applications to Polyenes C_4H_6 to $C_{22}H_{24}$. *J. Chem. Phys.* **1988**, *89*, 385−395.
(102) Toto, J. L.; Toto, T. T.; de Melo, C. P.; Kirtman, B.; Robins, K. Hartree−Fock Static Longitudinal (Hyper)polarizability of Polyyne. *J. Chem. Phys.* **1996**, *104*, 8586−8592.
(103) Alparone, A. Theoretical Study of the Electronic (Hyper)-polarizabilities of Amino Acids in Gaseous and Aqueous Phases. *Comput. Theor. Chem.* **2011**, *976*, 188−190.
(104) Alparone, A. Corrigendum to "Theoretical Study of the Electronic (Hyper)polarizabilities of Amino Acids in Gaseous and Aqueous Phases" [Comput. Theor. Chem. 976 (2011) 188−190]. *Comput. Theor. Chem.* **2012**, *980*, 144−144.
(105) Nakano, M.; Shigemoto, I.; Yamada, S.; Yamaguchi, K. Size-Consistent Approach and Density Analysis of Hyperpolarizability: Second Hyperpolarizabilities of Polymeric Systems with and without Defects. *J. Chem. Phys.* **1995**, *103*, 4175−4191.
(106) Yamada, S.; Nakano, M.; Yamaguchi, K. Structure−Property Correlation in the Second Hyperpolarizabilities γ for Phenyl Nitronyl Nitroxide Radicals. *Chem. Phys. Lett.* **1997**, *276*, 375−380.
(107) Nakano, M.; Yamada, S.; Yamaguchi, K. On the Second Hyperpolarizabilities γ of Three Charged States of Tetrathiapentalene and Tetrathiafulvalene: a γ Density Analysis. *Chem. Phys. Lett.* **2000**, *321*, 491−497.
(108) Jackson, K. A.; Yang, M.; Chaudhuri, I.; Frauenheim, T. Shape, Polarizability, and Metallicity in Silicon Clusters. *Phys. Rev. A* **2005**, *71*, 033205−.
(109) Karamanis, P.; Leszczynski, J. Correlations between Bonding, Size, and Second Hyperpolarizability (γ) of Small Semiconductor Clusters: Ab Initio Study on Al_nP_n Clusters with n = 2, 3, 4, 6, and 9. *J. Chem. Phys.* **2008**, *128*, 154323.
(110) Singh, U. C.; Kollman, P. A. An Approach to Computing Electrostatic Charges for Molecules. *J. Comput. Chem.* **1984**, *5*, 129−145.
(111) Besler, B. H.; Merz, K. M., Jr.; Kollman, P. A. Atomic Charges Derived from Semiempirical Methods. *J. Comput. Chem.* **1990**, *11*, 431−439.